Letter

Localization-driven quantum sensing

Ayan Sahoo,[1] Utkarsh Mishra,[2,3,*] and Debraj Rakshit[1]

[1]*Harish-Chandra Research Institute, A CI of Homi Bhabha National Institute, Chhatnag Road, Jhunsi, Allahabad 211 019, India*

[2]*Institute of Fundamental and Frontier Sciences, University of Electronic Science and Technology of China, Chengdu 610054, China*

[3]*Department of Physics and Astrophysics, University of Delhi, New Delhi 110007, India*

(Received 15 June 2023; accepted 2 January 2024; published 6 March 2024)

We show that the delocalization-localization transition in quantum many-body (QMB) systems are a compelling quantum resource for achieving quantum-enhanced sensitivity in parameter estimation. We exploit the vulnerability of a near-transition QMB state against the parameter shift for devising efficient sensing tools. In this realm the main focus of this work is to identify, propose, and analyze experimentally relevant quantum observables for precision measurement. Taking a QMB system as a Fermi lattice under quasiperiodic modulation that supports an energy-independent delocalization-localization transition, we suggest operator-based adiabatic and dynamical quantum sensors endowed with considerable quantum advantages. In particular, we analyze single-particle systems and the system at half-filling. While the quantum Fisher information saturates the Heisenberg limit, we demonstrate the experimentally relevant suitable observables with a spotlight on the charge-density-wave operator. Demonstrating their efficacy, these observables emerge as promising candidates for experimentally exploiting quantum advantages, showcasing superior performance compared to the standard quantum limit in terms of system-size scaling. Taking our exploration further into the dynamical realm, we discuss observables that yield super-extensive generic scaling in measurement precision. The comprehensive nature of our study not only sheds light on the intricacies of the delocalization-localization transition, but also offers practical insights for the development of quantum sensors and their potential applications.

DOI: 10.1103/PhysRevA.109.L030601

Introduction and motivation. There are ongoing efforts to propose and engineer robust physical systems for quantum sensing. Successful experimental efforts addressing quantum-enhanced measurement precision in parameter sensing are atomic clocks [1,2], interferometry [3–5], magnetometry [6,7], and ultracold spectroscopy [8,9]. The ultimate limit of precision in parameter estimation is given by the quantum Cramér-Rao bound [10–13]. The bound relates uncertainty $\mathcal{E}_q$ in the estimation of an unknown parameter with the quantum Fisher information (QFI) F_Q as $\mathcal{E}_q \geqslant (MF_Q)^{-1}$, where M is the number of repetition of the sensing protocol. QFI can reach the Heisenberg limit (HL), i.e., $F_Q \sim L^2$, for certain nonclassical quantum states with L qubits, whereas it scales linearly with system size, $F_Q \sim L$, known as the standard quantum limit (SQL), for L independent qubits [14,15].

Quantum metrology covers a wide gamut of research topics, starting from fundamental studies to applications in quantum technology [16–21]. Recently, a new class of quantum sensing devices, termed adiabatic sensors, have surfaced. They exploit cooperative quantum phenomena in isolated quantum many-body systems, such as quantum phase transitions [22–24], for achieving Heisenberg scaling [16,24–45]. The motivation of exploring criticality for sensing stems from the fact that around the critical point the macroscopic quantum state changes drastically even with a small change in the parameter characterizing the external signal. It is worth mentioning here that such an approach of sensing has been employed for classical systems [46]. Other kinds of quantum phase transition beyond the Landau theory of spontaneous symmetry breaking can also be advantageous, e.g., topological transitions [47], for achieving quantum-enhanced sensing [48]. In this realm, the localization-delocalization transition also harbors an enormous potential for quantum-enhanced parameter sensing, which this Letter explores. The self-dual symmetry of the Aubry-André-Harper (AAH) [49] model with quasiperiodic modulation leads to a localization transition as a finite modulation strength, V_c. Further works have confirmed the existence of a many-body localization transition in the presence of weak interactions [50,51]. There the quantum fidelity susceptibility at the transition point scales as $L^{2/(d\nu)}$ [52,53], where d denotes spatial dimension and the scaling exponent ν is associated with the localization length that scales as $\zeta \sim |V - V_c|^{-\nu}$ with $\nu = 1$ [54–56]. It immediately implies that the sensitivity of the unknown parameter V scales as $L^{2/(d\nu)}$ at the transition point. However, as it is challenging to experimentally access the fidelity between neighboring quantum states in quantum many-body (QMB) systems [57–59], the fidelity-based theoretical understanding does not promise an experimental translation [60]. Moreover, although a suitably optimized quantum operator, the evaluation of which generally turns out to be nontrivial within the many-body setting, can, in principle, saturate the maximum allowed precision governed by the QFI; it often transpires to be experimentally irrelevant [25]. Instead, we need to focus on experimentally accessible observables that may overcome the

*Present address: Ming Hsieh Department of Electrical and Computing Engineering, University of Southern California, Los Angeles, CA 90089, USA.

shot-noise limit (SNL) by a sizable amount and provide a substantial quantum advantage. We wish to mention here that a very recent work on Stark localization [61], which belongs to a different universality class, has been proposed for quantum-enhanced sensing, where the work is primarily focused on single-particle aspects of QFI [62]. Moreover, we resort to dynamical sensing protocols via sudden quench to encode the unknown parameter V in the probe state. Here the protocol duration time t manifests itself as a fundamental resource for the QFI scaling, along with the system size L. Similar to the adiabatic considerations, sensing protocols have been designed via non-equilibrium dynamics [63–66] influenced by criticality corresponding to a second-order quantum phase transition [24,27,29,31,67–70]. In particular, under certain assumptions, the dynamical precision quantified via QFI can at most scale as L^2t^2, where t represents total interrogation time [28,44,71]. This is the so-called HL in the dynamical context [14,15]. The dynamical sensors have certain advantages over the adiabatic counterparts, e.g., offering the protocol time as an additional resource for the scaling, overcoming the obstacles of critical slowing down, or designing better sensing protocols via the sudden quench strategy in comparison to the finite-time ramp required for implementing adiabatic protocols in reality [70,72]. Moreover, the measurement precision associated with an observable may attain a super-extensive growth with respect to the interrogation time, which is beyond the quadratic scaling of QFI, while perfectly respecting the allowed Cramér-Rao bounds.

Parameter estimation. Here we provide the essential background for estimating a single unknown parameter, V. We consider that the parameter is encoded either in the ground state or time-evolved state of a QMB system. As the parameter V changes locally, its fluctuation is captured by the fidelity susceptibility χ_Q, defined by

$$\chi_Q = -\lim_{\delta V\to 0}\frac{\partial^2 \mathcal{F}_Q}{\partial(\delta V)^2}, \tag{1}$$

where $\mathcal{F}_Q = \langle\psi(V)|\psi(V+\delta V)\rangle$ is the quantum fidelity between two nearby quantum states $|\psi(V)\rangle$ and $|\psi(V+\delta V)\rangle$. The fidelity susceptibility is related to the QFI as $F_Q = 4\chi_Q$ [25]. In general, one can infer the unknown parameter from the state $|\psi(V)\rangle$ by measuring an observable, $\hat{O}$. In the asymptotic limit, one can associate observable Fisher information (OFI) F_O, which is quantified by the error propagation formula following from the inverse of signal-to-noise ratio (SNR), as [24,73]

$$F_O^{-1} = \lim_{\delta V\to 0}\frac{\langle\hat{O}^2\rangle - \langle\hat{O}\rangle^2}{\left(\frac{d\langle\hat{O}\rangle}{d(\delta V)}\right)^2}. \tag{2}$$

The quantum Cramér-Rao bound [10] provides the bound on the uncertainty for any observable estimation: $F_O(V,\hat{O}) \leqslant F_Q(V)$ [12,13,73]. In the rest of the present Letter, we exploit the delocalization-localization transition, identify experimentally accessible observables with quantum advantage, and propose schemes for designing adiabatic and dynamical quantum sensors.

System. We study a one-dimensional fermionic lattice with an underlying quasiperiodically modulated onsite potential. The generic form of the Hamiltonian in the context of single-parameter estimation is $\hat{H}=\hat{H}_1 + V\hat{H}_2$. For the system under consideration, H_2 represents a quasiperiodically modulated onsite potential. Let us consider the single-particle limit first, where H_1 has a contribution only from the kinetic energy, $\hat{H}_1 \equiv \hat{H}_{ke}$. In this case the final Hamiltonian is given by

$$\hat{H} = -\sum_i(\hat{c}_i^\dagger\hat{c}_{i+1} + \text{H.c.}) + V\sum_i \cos(2\pi i\omega)\hat{c}_i^\dagger\hat{c}_i, \tag{3}$$

where ω is an irrational number, and $\hat{c}_i^\dagger(\hat{c}_i)$ is a fermionic creation (annihilation) operator at the ith site. The Hamiltonian represents the AAH model, which has been studied in various contexts, such as the Hofstadter butterfly [74], transport [75,76], mobility edge [77–79], criticality [54,80,81], and topological phases [82–84]. The AAH model has a self-dual symmetry between the Hamiltonians in the momentum and the position space, which leads to an energy-independent localization transition at a finite modulation strength, $V_c = 2$. For a given V, all the states are either localized (for $V > V_c$) or extended (for $V < V_c$). However, we restrict our interest to the localization transition in the ground state and examine its usefulness for adiabatic sensing. Due to the fractal nature and even-odd dichotomy, the system is not typical because all system sizes cannot fit under the same scaling functions [54,85]. For finite-size systems, proper scaling emerges at the transition for system sizes F_n with either odd or even sequences from the Fibonacci series and for ω to be approximated by $\omega_n = F_n/F_{n+1}$. Here F_n and F_{n+1} are two consecutive Fibonacci numbers with the property $\omega = \lim_{n\to\infty}(F_n/F_{n+1}) \to (\sqrt{5}-1)/2$, which is the so-called golden ratio. This work considers periodic boundary conditions (PBCs), odd lattice sizes, and scaling at the transition point. Experimental observations of localization transition in the AAH model have been reported, e.g., in the ultracold atom setup [86–90] and in photonic crystals [91–94].

In addition to the single-particle case, we study the half-filled case in the presence of interaction. $\hat{H}_1$ gets modified as $\hat{H}_1 = \hat{H}_{ke} + \hat{H}_{\text{int}}$, where we choose to keep the interaction term simple nearest-neighbor type, such that

$$\hat{H}_{\text{int}} = U\sum_i \hat{n}_i\hat{n}_{i+1}, \tag{4}$$

where $\hat{n}_i = \hat{c}_i^\dagger\hat{c}_i$, and U is the interaction strength.

The localization transition persists in the ground state in the presence of interaction [95,96]. Moreover, further theoretical works have argued in favor of many-body localization (MBL) [50,51,97–99], albeit with different universality properties than the uncorrelated disordered system.

Single-particle case: Adiabatic. The QFI, defined via Eq. (1), saturates the HL, i.e., it scales quadratically with the system size: $F_Q^*(V=V^*)\sim L^2$, where V^* corresponds to quasiperiodic potential amplitude for which QFI maximizes. It reveals the potential of the AAH-type many-body Hamiltonian to be exploited for building a new class of quantum sensing devices. We now need to identify experimentally accessible observables endowed with a quantum advantage.

We focus on an observable that measures the occupation imbalance between the even and odd sites. The corresponding operator is $\hat{O}_{\text{cdw}} = \sum_i(-1)^i\hat{c}_i^\dagger\hat{c}_i/n_f$, which reveals the charge-density-wave (CDW) order in a quantum state. For in-

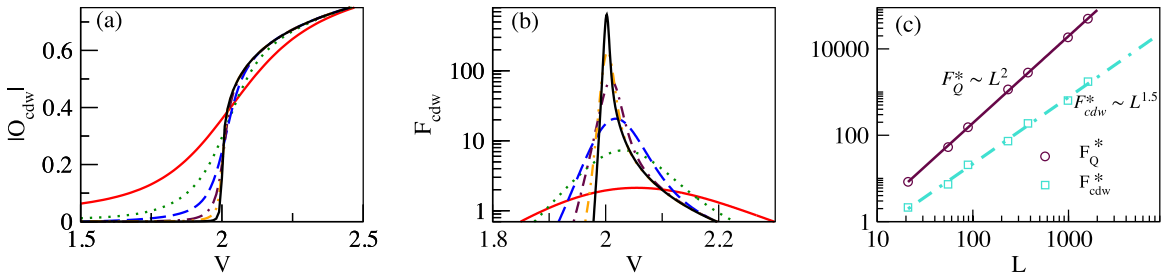

FIG. 1. Single-particle case: (a) Modulus of $|O_{\rm cdw}|$ as a function of V for $L = 21$ (solid red), 55 (dotted), 89 (dashed), 233 (dashed-dotted), 377 (dashed-dotted-dotted), and 987 (solid black). The inflation points (V^*) corresponding to different L approach the transition point V_c in the thermodynamic limit. (b) OFI ($F_{\rm cdw}$) corresponding to the operator $\hat{O}_{\rm cdw}$ as a function of V for the same set of system sizes presented in (a). The localization transition point at $V_c = 2$ is marked by the gradual prominence of the OFI peaks with increasing lattice sites. The plot styles are kept consistent. (c) The circles and the squares show the maximum QFI, F_Q^*, and maximum OFI, $F_{\rm cdw}^*$, at V^* as a function of the L. The straight line show the best fits for F_Q^* (solid line) and F_{cwd}^* (dashed line). QFI admits Heisenberg scaling, i.e., $F_Q^* \sim L^2$. The best fit is shown by the dashed straight line that reveals $F_{\rm cdw}^* \sim L^{1.5}$.

stance, this operator is directly measurable within the optical lattice setup loaded with ultracold atoms [86]. We consider system size up to $L = 1597$. The computation of OFI, as followed from Eq. (2), requires evaluation of the expectation values of $\langle \hat{O}_{\rm cdw} \rangle$, $\langle \hat{O}_{\rm cdw}^2 \rangle$, where $\hat{O}_{\rm cdw}^2 = \sum_{i,j} (-1)^{i+j} \hat{n}_i \hat{n}_j$. From now on, we switch to a more convenient notation for the operator expectation value: $O_\alpha \equiv \langle \hat{O}_\alpha \rangle$. Figure 1(a) shows the modulus of the charge-density order $|O_{\rm cdw}|$ as a function of the amplitude of the potential V. Due to the extended nature of the quantum state, $O_{\rm cdw}$ gradually diminishes with increasing L in the delocalized phase but acquires a finite value in the localized phase. This feature, as expected, becomes sharper with increasing system size and proceeds to assume a step-function-like structure with vanishing $|O_{\rm cdw}|$ in the extended phase in the thermodynamic limit. The inflation points corresponding to different system sizes tend to converge towards the infinite system transition point, $V_c = 2$. Figure 1(b) shows the OFI, $F_{\rm cdw}$, corresponding to the various system sizes as a function of V. The $F_{\rm cdw}$ develops a peak at finite-size transition points, V^*. They are characterized via gradual prominence of the peaks at near V_c. While the QFI at the transition point, F_Q^*, admits a scaling of $F_Q^* = L^{2.01(1)}$, the OFI at the transition point, $F_{\rm cdw}^*$, scales like $F_{\rm cdw}^* = L^{1.54(4)}$ [see Fig. 1(c)]. The scaling associated with $F_{\rm cdw}^*$ is less than the HL limit but comfortably beats the SNL, hence offering a genuine quantum advantage in the measurement precision.

Half-filled case: Adiabatic. We now turn our attention to the half-filled case, i.e., the number of fermions is $(L \pm 1)/2$ [100], with PBC. We perform density matrix renormalization group (DMRG) calculations via matrix product state (MPS) formalism for the interacting systems [101,102]. We probe the ground state F_Q for system sizes up to $L = 1597$ ($n_f = 798$) for the noninteracting (NI) cases and up to $L = 89$ ($n_f = 45$) in the interacting cases [103]. The influence of interaction remains minimal on the scaling properties for weak to moderate interaction strengths [103].

Figure 2(a) presents F_Q as a function of V for different interaction strengths U and fixed L. We note two observations: First, the peak tends to shift towards a higher V^* with increasing U. This is expected, as many-body localization transition is supposed to occur at $V_c > 2$ in the presence of interaction. And second, the value of F_Q tends to slightly decrease at V^* with increasing U. The scaling of the QFI at V^*, F_Q^*, is presented in Fig. 2(b). F_Q^* scales as $F_Q^*(U = 0) = L^{1.98(2)}$ in the NI limit, i.e., it saturates the HL limit. Despite the lack of enough data points, it is evident that the effects of interaction on the scaling exponent remain pretty small in the range of weak to intermediate range. For the case shown here, QFI also nearly saturates the HL limit: $F_Q^*(U = 1.2) = L^{1.95(4)}$.

Proposing an experimentally relevant observable with quantum advantage for the fractionally filled equilibrium case turns out to be nontrivial. The operator $\hat{O}_{\rm cdw}$ is not a suitable operator, as the ground state is devoid of CDW (charge-hole) ordering in the localized phase [100]. Unlike the single-particle case, it fails to characterize the transition, and no proper scaling with L is found. However, a proper scaling can be found with other suitable observables, such as $\hat{O}_{H_2} = \sum_i \cos(2\pi i\omega) \hat{c}_i^\dagger \hat{c}_i$ (which is basically $\hat{H}_2$, but a new notation has been introduced for consistency: $\hat{O}_{H_2} \equiv \hat{H}_2$). The corresponding OFI (F_{H_2}), as followed from Eq. (2), admits a proper scaling with L, $F_{H_2}^* = L^{1.04(1)}$, but it barely beats the SQL. One may think of a few strategies, one of which is preparing the system artificially in a highly excited state with high CDW order and then monitoring the adiabatic evolution of $\hat{O}_{\rm cdw}$ by tuning V to lower values. This strategy, however, may not be useful because of closely lying, near-degenerate excited states or energy crossings. The second way is to adopt a dynamical strategy for engineering dynamical sensors. The protocol is to prepare the system in the ground or highly excited state with high CDW order and then quench to or through V_c to either of the phases.

Half-filled case: Dynamics. Two specific schemes are considered: Performing a sudden quench from an initial state, $|\psi_{in}\rangle$, which can be (1) the ground state corresponding to a particular phase, or (2) a state with maximum CDW order ($O_{\rm cdw} = 1$), e.g., $|1010\cdots\rangle$, which is a high excited state of the system in the limit $V \to \infty$. Such a high CDW state can be prepared artificially with high fidelity, e.g., in ultracold atom experiments [86]. A further scheme to construct QFI runs as follows: (i) Pump a continuous resource for a specific duration, t, via unitary dynamics provided by a driving Hamiltonian, $\hat{H}(V_f)$, (ii) back-propagate the evolved state,

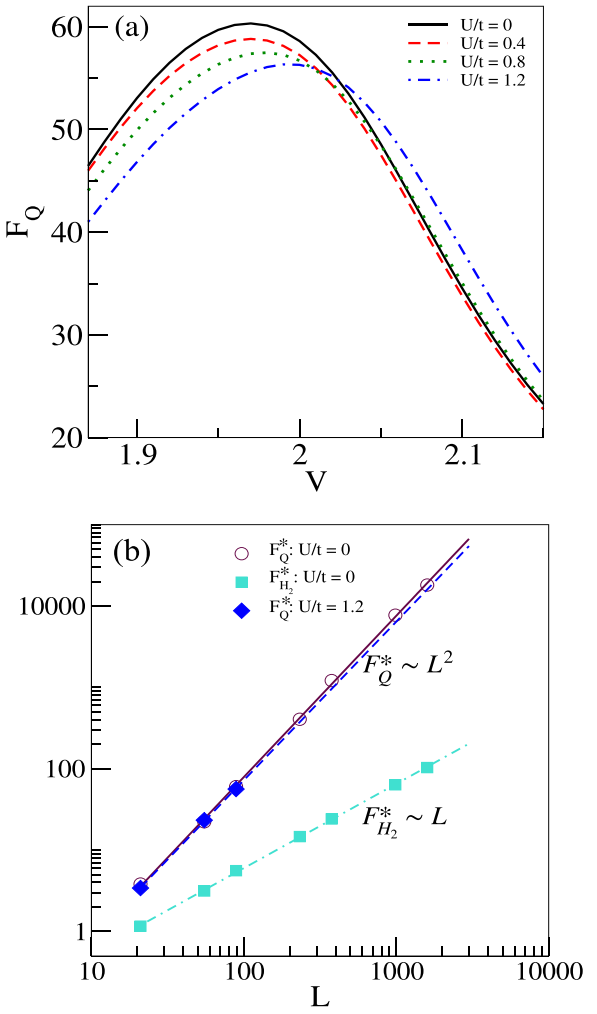

FIG. 2. Half-filled case – Adiabatic: (a) Interaction effects for particular case at half-filling ($L = 89$ and $n_f = 45$). The plot shows F_Q as a function of V for varied interaction strengths (up to the interaction strength comparable to the kinetic energy). (b) The maximum QFI, F_Q^*, and OFI, $F_{\mathrm{H}_2}^*$, corresponding to a natural operator $\hat{H}_2$ as a function of L for $U = 0$. The number of fermions n_f for $L = 21$, 55, 89, 233, 377, 987, and 1597 are 11, 28, 45, 116, 189, 494, and 798, respectively. While F_Q^* nearly saturates the Heisenberg limit, i.e., $F_Q^* \sim L^2$ for both, the bare system and a system with moderate interaction ($U = 1.2$, represented via diamonds), $F_{\mathrm{H}_2}^*$ scales linearly with L and hence only saturates the SQL.

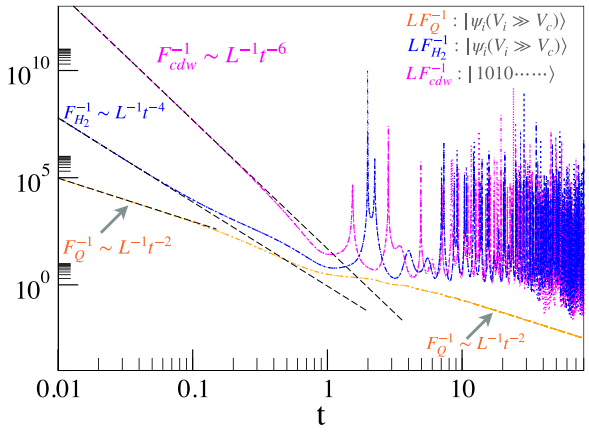

FIG. 3. Half-filled case – Dynamics: Time dependence of QFI and OFI due to a sudden quench in V ($U = 0$) for L =55 (dot-dot), 89 (dash-dot), and 233 (dash-dot-dot). Collapse plots of the inverse of the quantities are presented after rescaling them with L^α. Considering an initial state as the ground state prepared in the localized phase (case shown is for $V = 5$), the figure shows scaled QFI (orange lines). The scaled data set collapses for $\alpha = 1$, implying $F_Q \sim Lt^2$. OFI (F_{H_2}), presented for the same initial state, scales as $F_{H_2} \sim Lt^4$ (blue lines) at short or transient time. Finally, the OFI, F_{cdw}, corresponding to an initial state with maximum CDW order is shown to scale like $F_{\mathrm{cdw}} \sim Lt^6$ (magenta lines) for $t \lesssim 1$. Data corresponding to different L merge on top of each other, and the naked eye may be unable to differentiate them.

$|\psi(V_f, t)\rangle$, with the Hamiltonian $\hat{H}_f(V_f + \delta V)$, and (iii) the back-propagated state is projected on the initial state in order to obtain the fidelity, $\mathcal{F}(t) = \langle\psi(V, t)|\psi(V + \delta V, t)\rangle$. Importantly, as there may be an experimental limitation on time due to decoherence, the observables' short- or transient-time behavior is of prime interest.

We illustrate the time dependence of the QFIs and OFIs calculated under the above-mentioned situations in Fig. 3 for $U = 0$ and different system sizes $L = 55$, 89, and 233 at half-filling. We plot the inverse of the quantities under consideration and rescale them with L. Data sets corresponding to different L's collapse quite well, implying a saturation in the SNL as a function of L. In Fig. 3 we show F_Q^{-1} and $F_{H_2}^{-1}$ for the initial state, $|\psi_{in}(V \gg V_c)\rangle$, as the ground state prepared in the localized phase and then driven to the extended phase. While F_Q overall scales as $\sim Lt^2$ in the short and long times [104–107], two characteristic timescales emerge in OFIs. At short/transient time, roughly up to $t \sim 1$, F_{H_2} assumes a higher scaling in t: $F_{H_2} = Lt^{3.92(1)}$. The observables exhibit rapid oscillations at $t \gtrsim 1$. We find the long-time average value to have a roughly quadratic scaling in time. However, $\hat{O}_{\mathrm{cdw}}$ holds prime interest, as described in the context of adiabatic sensors. Considering the charge-hole ordered state $|1010\cdots\rangle$ as the initial state, the dynamics allow us to circumvent the scaling issues associated with the adiabatic scenario. It even offers superior scaling in the transient time in comparison to F_{H_2}: $F_{\mathrm{cdw}} = Lt^{6.003(7)}$. Note that although the F_O exhibits a higher scaling than F_Q in transient time, the absolute value of F_O is upper bounded by F_Q, as expected. Remarkably, when the system is not prepared too close to the transition point, the dynamical scaling laws are quite generic, i.e., they are independent of the final driving Hamiltonian and the initial state [100].

Discussion. In this work we perform canonical equilibrium and dynamical studies of single-parameter quantum sensing via experimentally accessible natural observables in a quasiperiodically modulated, single-particle, and half-filled Fermi lattice. Important findings are the following: Within the adiabatic scenario, while the QFI can attain the HL limit in both the single-particle and half-filled cases, an experimentally accessible observable, CDW order ($\hat{O}_{\mathrm{cdw}}$), is proposed that is endowed with a significant quantum advantage at the localization transition in the single-particle limit. The same

observable, however, is not suitable in the half-filled case for the scaling analysis, as the typical ground-state configuration needs an important ingredient—the charge-hole ordering. Instead, the system can be initially prepared in a quantum state that maintains the required ordering and then can be quenched across or at the transition point. Remarkably, this provides a super-extensive *generic* (i.e., robust against the final driving Hamiltonian) scaling in the measurement precision. We also report another natural observable, $\hat{O}_{H_2}$, experimental access for which may be comparatively nontrivial, as it requires measurement of the fermionic occupation number at individual sites, which provides significant quantum advantages in precision measurement, even if the system is initially prepared in the ground state. In conclusion, we propose the localization-delocalization transition as a resource that can be exploited for engineering a new class of quantum sensors. This idea brings the scope for exercising further exciting investigations, e.g., in the context of multiparameter sensing, sensing via partial accessibility, or sensing via localization induced by uncorrelated disorder.

Acknowledgments. D.R. acknowledges support from the Science and Engineering Research Board (SERB), Department of Science and Technology (DST), Government of India, under Sanction No. SRG/2021/002316-G. U.M. acknowledges support from the Institute of Eminence (IoE), University of Delhi, through the Faculty Research Program (FRP) grants, sanctioned under No. IoE/2023-24/12/FRP.

[1] J. Appel, P. J. Windpassinger, D. Oblak, U. B. Hoff, N. Kjaergaard, and E. S. Polzik, Mesoscopic atomic entanglement for precision measurements beyond the standard quantum limit, Proc. Natl. Acad. Sci. USA **106**, 10960 (2009).

[2] A. Louchet-Chauvet, J. Appel, J. J. Renema, D. Oblak, N. Kjaergaard, and E. S. Polzik, Entanglement-assisted atomic clock beyond the projection noise limit, New J. Phys. **12**, 065032 (2010).

[3] M. W. Mitchell, J. S. Lundeen, and A. M. Steinberg, Super-resolving phase measurements with a multi-photon entangled state, Nature (London) **429**, 161 (2004).

[4] T. Nagata, R. Okamoto, J. L. O'Brien, K. Sasaki, and S. Takeuchi, Beating the standard quantum limit with four entangled photons, Science **316**, 726 (2007).

[5] LIGO Collaboration, A gravitational wave observatory operating beyond the quantum shot-noise limit, Nat. Phys. **7**, 962 (2011); Enhanced sensitivity of the LIGO gravitational wave detector by using squeezed states of light, Nat. Photonics **7**, 613 (2013).

[6] W. Wasilewski, K. Jensen, H. Krauter, J. J. Renema, M. V. Balabas, and E. S. Polzik, Quantum noise limited and entanglement-assisted magnetometry, Phys. Rev. Lett. **104**, 133601 (2010).

[7] R. J. Sewell, M. Koschorreck, M. Napolitano, B. Dubost, N. Behbood, and M. W. Mitchell, Magnetic sensitivity beyond the projection noise limit by spin squeezing, Phys. Rev. Lett. **109**, 253605 (2012).

[8] D. Leibfried, M. D. Barrett, T. Schaetz, J. Britton, J. Chiaverini, W. M. Itano, J. D. Jost, C. Langer, and D. J. Wineland, Toward Heisenberg-limited spectroscopy with multiparticle entangled states, Science **304**, 1476 (2004).

[9] C. F. Roos, M. Chwalla, K. Kim, M. Riebe, and R. Blatt, Designer atoms for quantum metrology, Nature (London) **443**, 316 (2006).

[10] S. L. Braunstein and C. M. Caves, Statistical distance and the geometry of quantum states, Phys. Rev. Lett. **72**, 3439 (1994).

[11] C. L. Degen, F. Reinhard, and P. Cappellaro, Quantum sensing, Rev. Mod. Phys. **89**, 035002 (2017).

[12] H. Cramér, *Mathematical Methods of Statistics* (Princeton University Press, Princeton, NJ, 1946).

[13] C. W. Helstrom, *Quantum Detection and Estimation Theory* (Academic Press, New York, 1976).

[14] V. Giovannetti, S. Lloyd, and L. Maccone, Quantum-enhanced measurements: Beating the standard quantum limit, Science **306**, 1330 (2004).

[15] V. Giovannetti, S. Lloyd, and L. Maccone, Quantum metrology, Phys. Rev. Lett. **96**, 010401 (2006).

[16] L. Pezzé, A. Smerzi, M. K. Oberthaler, R. Schmied and P. Treutlein, Quantum metrology with nonclassical states of atomic ensembles, Rev. Mod. Phys. **90**, 035005 (2018).

[17] S. F. Huelga, C. Macchiavello, T. Pellizzari, A. K. Ekert, M. B. Plenio, and J. I. Cirac, The improvement of frequency standards with quantum entanglement, Phys. Rev. Lett. **79**, 3865 (1997).

[18] M. Oszmaniec, R. Augusiak, C. Gogolin, J. Kołodyński, A. Acín, and M. Lewenstein, Random bosonic states for robust quantum metrology, Phys. Rev. X **6**, 041044 (2016).

[19] H. Zhou, J. Choi, S. Choi, R. Landig, A. M. Douglas, J. Isoya, F. Jelezko, S. Onoda, H. Sumiya, P. Cappellaro, H. S. Knowles, H. Park, and M. D. Lukin, Quantum metrology with strongly interacting spin systems, Phys. Rev. X **10**, 031003 (2020).

[20] J. Naikoo, R. W. Chhajlany, and J. Kołodyński, Multiparameter estimation perspective on non-Hermitian singularity-enhanced sensing, Phys. Rev. Lett. **131**, 220801 (2023).

[21] A. Bhattacharyya, A. Ghoshal, and U. Sen, Restoring metrological quantum advantage of measurement precision in noisy scenario, arXiv:2211.05537.

[22] S. Sachdev, *Quantum Phase Transitions* (Cambridge University Press, Cambridge, England, 1999).

[23] A. Dutta, G. Aeppli, B. K. Chakrabarti, U. Divakaran, T. F. Rosenbaum, and D. Sen, *Quantum Phase Transitions in Transverse Field Spin Models: From Statistical Physics to Quantum Information* (Cambridge University Press, Cambridge, England, 2015).

[24] M. M. Rams, P. Sierant, O. Dutta, P. Horodecki, and J. Zakrzewski, At the limits of criticality-based quantum metrology: Apparent super-Heisenberg scaling revisited, Phys. Rev. X **8**, 021022 (2018).

[25] P. Zanardi, M. G. Paris, and L. C. Venuti, Quantum criticality as a resource for quantum estimation, Phys. Rev. A **78**, 042105 (2008).

[26] L. C. Venuti and P. Zanardi, Quantum critical scaling of the geometric tensors, Phys. Rev. Lett. **99**, 095701 (2007).

[27] M. Tsang, Quantum transition-edge detectors, Phys. Rev. A **88**, 021801(R) (2013).

[28] L. Garbe, M. Bina, A. Keller, M. G. Paris, and S. Felicetti, Critical quantum metrology with a finite-component quantum phase transition, Phys. Rev. Lett. **124**, 120504 (2020).

[29] U. Mishra and A. Bayat, Driving enhanced quantum sensing in partially accessible many-body systems, Phys. Rev. Lett. **127**, 080504 (2021).

[30] K. Gietka, F. Metz, T. Keller, and J. Li, Adiabatic critical quantum metrology cannot reach the Heisenberg limit even when shortcuts to adiabaticity are applied, Quantum **5**, 489 (2021).

[31] Y. Chu, S. Zhang, B. Yu, and J. Cai, Dynamic framework for criticality-enhanced quantum sensing, Phys. Rev. Lett. **126**, 010502 (2021).

[32] M. Salado-Mejía, R. Román-Ancheyta, F. Soto-Eguibar, and H. Moya-Cessa, Spectroscopy and critical quantum thermometry in the ultrastrong coupling regime, Quantum Sci. Technol. **6**, 025010 (2021).

[33] L. Pezzé and L. Lepori, Robust multipartite entanglement in dirty topological wires, arXiv:2204.02209.

[34] V. Montenegro, U. Mishra, and A. Bayat, Global sensing and its impact for quantum many-body probes with criticality, Phys. Rev. Lett. **126**, 200501 (2021).

[35] R. Di Candia, F. Minganti, K. Petrovnin, G. Paraoanu, and S. Felicetti, Critical parametric quantum sensing, NPJ Quantum Inf. **9**, 23 (2023).

[36] S. S. Mirkhalaf, E. Witkowska, and L. Lepori, Supersensitive quantum sensor based on criticality in an antiferromagnetic spinor condensate, Phys. Rev. A **101**, 043609 (2020).

[37] L. Pezzé and A. Smerzi, Quantum theory of phase estimation in atom interferometry, in *Proceedings of the International School of Physics Enrico Fermi*, Course 188, Varenna, edited by G. M. Tino and M. A. Kasevich (IOS Press, Amsterdam, 2016), p. 691.

[38] I. Frérot and T. Roscilde, Quantum critical metrology, Phys. Rev. Lett. **121**, 020402 (2018).

[39] P. Zanardi and N. Paunković, Ground state overlap and quantum phase transitions, Phys. Rev. E **74**, 031123 (2006).

[40] W.-L. You, Y.-W. Li, and S.-J. Gu, Fidelity, dynamic structure factor, and susceptibility in critical phenomena, Phys. Rev. E **76**, 022101 (2007).

[41] P. Zanardi, P. Giorda, and M. Cozzini, Information-theoretic differential geometry of quantum phase transitions, Phys. Rev. Lett. **99**, 100603 (2007).

[42] S.-J. Gu, Fidelity approach to quantum phase transitions, Int. J. Mod. Phys. B **24**, 4371 (2010).

[43] D. Braun, G. Adesso, F. Benatti, Ro. Floreanini, U. Mar-zolino, M. W. Mitchell, and S. Pirandola, Quantum-enhanced measurements without entanglement, Rev. Mod. Phys. **90**, 035006 (2018).

[44] T. Ilias, D. Yang, S. F. Huelga, and M. B. Plenio, Criticality-enhanced quantum sensing via continuous measurement, PRX Quantum **3**, 010354 (2022).

[45] D. Yang, S. F. Huelga, and M. B. Plenio, Efficient information retrieval for sensing via continuous measurement, Phys. Rev. X **13**, 031012 (2023).

[46] K. Irwin and G. Hilton, in *Cryogenic Particle Detection, Topics in Applied Physics*, edited by C. Enss (Springer Berlin Heidelberg, 2005), pp. 63–150.

[47] B. A. Bernevig, *Topological Insulators and Topological Superconductors* (Princeton University Press, Princeton, NJ, 2013).

[48] S. Sarkar, C. Mukhopadhyay, A. Alase, and A. Bayat, Free-fermionic topological quantum sensors, Phys. Rev. Lett. **129**, 090503 (2022).

[49] S. Aubry and G. André, Anderson localization for one-dimensional difference Schrödinger operator with quasiperiodic potential, Ann. Isr. Phys. Soc. **3**, 18 (1980).

[50] V. P. Michal, B. L. Altshuler, and G. V. Shlyapnikov, Delocalization of weakly interacting bosons in a 1D quasiperiodic potential, Phys. Rev. Lett. **113**, 045304 (2014).

[51] S. Iyer, V. Oganesyan, G. Refael, and D. A. Huse, Many-body localization in a quasiperiodic system, Phys. Rev. B **87**, 134202 (2013).

[52] M. Thakurathi, D. Sen, and A. Dutta, Fidelity susceptibility of one-dimensional models with twisted boundary conditions, Phys. Rev. B **86**, 245424 (2012).

[53] T. Cookmeyer, J. Motruk, and J. E. Moore, Critical properties of the ground-state localization-delocalization transition in the many-particle Aubry-André model, Phys. Rev. B **101**, 174203 (2020).

[54] B.-Bo Wei, Fidelity susceptibility in one-dimensional disordered lattice models, Phys. Rev. A **99**, 042117 (2019).

[55] A. Sinha, M. M. Rams, and J. Dziarmaga, Kibble-Zurek mechanism with a single particle: Dynamics of the localization-delocalization transition in the Aubry-André model, Phys. Rev. B **99**, 094203 (2019).

[56] X. Bu, L.-J. Zhai, and S. Yin, Quantum criticality in the disordered Aubry-André model, Phys. Rev. B **106**, 214208 (2022).

[57] S.-J. Gu and W. C. Yu, Spectral function and fidelity susceptibility in quantum critical phenomena, Europhys. Lett. **108**, 20002 (2014).

[58] J. Zhang, X. Peng, N. Rajendran, and D. Suter, Detection of quantum critical points by a probe qubit, Phys. Rev. Lett. **100**, 100501 (2008).

[59] J. Zhang, F. M. Cucchietti, C. M. Chandrashekar, M. Laforest, C. A. Ryan, M. Ditty, A. Hubbard, J. K. Gamble, and R. Laflamme, Direct observation of quantum criticality in Ising spin chains, Phys. Rev. A **79**, 012305 (2009).

[60] M. Cerezo, A. R. Poremba, L. Cincio, and P. J. Coles, Variational quantum fidelity estimation, Quantum **4**, 248 (2020).

[61] G. H. Wannier, Wave functions and effective Hamiltonian for Bloch electrons in an electric field, Phys. Rev. **117**, 432 (1960).

[62] X. He, R. Yousefjani, and A. Bayat, Stark localization as a resource for weak-field sensing with super-Heisenberg precision, Phys. Rev. Lett. **131**, 010801 (2023).

[63] A. Polkovnikov, K. Sengupta, A. Silva, and M. Vengalattore, Colloquium: Nonequilibrium dynamics of closed interacting quantum systems, Rev. Mod. Phys. **83**, 863 (2011).

[64] J. Eisert, M. Friesdorf, and C. Gogolin, Quantum many-body systems out of equilibrium, Nat. Phys. **11**, 124 (2015).

[65] V. Montenegro, G. S. Jones, S. Bose, and A. Bayat, Sequential measurements for quantum-enhanced magnetometry in spin chain probes, Phys. Rev. Lett. **129**, 120503 (2022).

[66] V. Montenegro, M. G. Genoni, A. Bayat, and M. G. A. Paris, Quantum-enhanced boundary time crystal sensors, Commun. Phys. **6**, 304 (2023).

[67] U. Mishra and A. Bayat, Integrable quantum many-body sensors for AC field sensing, Sci. Rep. **12**, 14760 (2022).

[68] K. Macieszczak, M. Guta, I. Lesanovsky, and J. P. Garrahan, Dynamical phase transitions as a resource for quantum enhanced metrology, Phys. Rev. A **93**, 022103 (2016).

[69] E. Torrontegui, S. Ibáñez, S. Mart'inez-Garaot, M. Modugno, A. del Campo, D. Gueŕy-Odelin, A. Ruschhaupt, X. Chen, and J. G. Muga, *Advances in Atomic, Molecular, and Optical Physics*, edited by E. Arimondo, P. R. Berman, and C. C. Lin (Academic Press, New York, 2013), Vol. 62, pp. 117–169.

[70] L. Garbe, O. Abah, S. Felicetti, and R. Puebla, Critical quantum metrology with fully-connected models: From Heisenberg to Kibble-Zurek scaling, Quantum Sci. Technol. **7**, 035010 (2022).

[71] S. Boixo, S. T. Flammia, C. M. Caves, and J. M. Geremia, Generalized limits for single-parameter quantum estimation, Phys. Rev. Lett. **98**, 090401 (2007).

[72] J. Yang, S. Pang, Z. Chen, A. N. Jordan, and A. del Campo, Variational principle for optimal quantum controls in quantum metrology, Phys. Rev. Lett. **128**, 160505 (2022).

[73] L. Pezzé, A. Trenkwalder, and M. Fattori, Adiabatic sensing enhanced by quantum criticality, arXiv:1906.01447.

[74] D. R. Hofstadter, Energy levels and wave functions of Bloch electrons in rational and irrational magnetic fields, Phys. Rev. B **14**, 2239 (1976).

[75] A. Purkayastha, S. Sanyal, A. Dhar, and M. Kulkarni, Anomalous transport in the Aubry-André-Harper model in isolated and open systems, Phys. Rev. B **97**, 174206 (2018).

[76] J. Sutradhar, S. Mukerjee, R. Pandit, and S. Banerjee, Transport, multifractality, and the breakdown of single-parameter scaling at the localization transition in quasiperiodic systems, Phys. Rev. B **99**, 224204 (2019).

[77] S. Saha, S. K. Maiti, and S. Karmakar, Multiple mobility edges in a 1D Aubry chain with Hubbard interaction in presence of electric field: Controlled electron transport, Physica E **83**, 358 (2016).

[78] S. Ganeshan, J. H. Pixley, and S. Das Sarma, Nearest neighbor tight binding models with an exact mobility edge in one dimension, Phys. Rev. Lett. **114**, 146601 (2015).

[79] X. Li, S. Ganeshan, J. H. Pixley, and S. Das Sarma, Many-Body localization and quantum nonergodicity in a model with a single-particle mobility edge, Phys. Rev. Lett. **115**, 186601 (2015).

[80] A. Szabó and U. Schneider, Non-power-law universality in one-dimensional quasicrystals, Phys. Rev. B **98**, 134201 (2018).

[81] R. Modak and D. Rakshit, Many-body dynamical phase transition in a quasiperiodic potential, Phys. Rev. B **103**, 224310 (2021).

[82] W. DeGottardi, D. Sen, and S. Vishveshwara, Majorana fermions in superconducting 1D systems having periodic, quasiperiodic, and disordered potentials, Phys. Rev. Lett. **110**, 146404 (2013).

[83] X. Cai, L.-J. Lang, S. Chen, and Y. Wang, Topological superconductor to Anderson localization transition in one-dimensional incommensurate lattices, Phys. Rev. Lett. **110**, 176403 (2013).

[84] J. Fraxanet, U. Bhattacharya, T. Grass, D. Rakshit, M. Lewenstein, and A. Dauphin, Topological properties of the long-range Kitaev chain with Aubry-André-Harper modulation, Phys. Rev. Res. **3**, 013148 (2021).

[85] J. C. C. Cestari, A. Foerster, M. A. Gusmaõ, and M. Continentino, Critical exponents of the disorder-driven superfluid-insulator transition in one-dimensional Bose-Einstein condensates, Phys. Rev. A **84**, 055601 (2011).

[86] M. Schreiber, S. S. Hodgman, P. Bordia, H. P. Lüschen, M. H. Fischer, R. Vosk, E. Altman, U. Schneider, and I. Bloch, Observation of many-body localization of interacting fermions in a quasirandom optical lattice, Science **349**, 842 (2015).

[87] L. D. Negro, C. J. Oton, Z. Gaburro, L. Pavesi, P. Johnson, A. Lagendijk, R. Righini, M. Colocci, and D. S. Wiersma, Light transport through the band-edge states of Fibonacci quasicrystals, Phys. Rev. Lett. **90**, 055501 (2003).

[88] G. Roati, C. D'Errico, L. Fallani, M. Fattori, C. Fort, M. Zaccanti, G. Modugno, M. Modugno, and M. Inguscio, Anderson localization of a non-interacting Bose-Einstein condensate, Nature (London) **453**, 895 (2008).

[89] G. Modugno, Anderson localization in Bose-Einstein condensates, Rep. Prog. Phys. **73**, 102401 (2010).

[90] The AAH model is particularly suitable for implementation via ultracold atoms in optical lattice by effectively freezing the dynamics in the two orthogonal directions by employing the deep lattice in those directions and introducing an additional detuning lattice that is much weaker in comparison to the primary lattice.

[91] Y. Lahini, R. Pugatch, F. Pozzi, M. Sorel, R. Morandotti, N. Davidson, and Y. Silberberg, Observation of a localization transition in quasiperiodic photonic lattices, Phys. Rev. Lett. **103**, 013901 (2009).

[92] Y. E. Kraus, Y. Lahini, Z. Ringel, M. Verbin, and O. Zilberberg, Topological states and adiabatic pumping in quasicrystals, Phys. Rev. Lett. **109**, 106402 (2012).

[93] M. Verbin, O. Zilberberg, Y. E. Kraus, Y. Lahini, and Y. Silberberg, Observation of topological phase transitions in photonic quasicrystals, Phys. Rev. Lett. **110**, 076403 (2013).

[94] M. Verbin, O. Zilberberg, Y. Lahini, Y. E. Kraus, and Y. Silberberg, Topological pumping over a photonic Fibonacci quasicrystal, Phys. Rev. B **91**, 064201 (2015).

[95] V. Mastropietro, Localization of interacting fermions in the Aubry-André model, Phys. Rev. Lett. **115**, 180401 (2015).

[96] V. Mastropietro, Localization in interacting fermionic chains with quasi-random disorder, Commun. Math. Phys. **351**, 283 (2017).

[97] V. Khemani, D. N. Sheng, and D. A. Huse, Two universality classes for the many-body localization transition, Phys. Rev. Lett. **119**, 075702 (2017).

[98] P. Naldesi, E. Ercolessi, and T. Roscilde, Detecting a many-body mobility edge with quantum quenches, SciPost Phys. **1**, 010 (2016).

[99] F. Setiawan, D.-L. Deng, and J. H. Pixley, Transport properties across the many-body localization transition in quasiperiodic and random systems, Phys. Rev. B **96**, 104205 (2017).

[100] See Supplemental Material at http://link.aps.org/supplemental/10.1103/PhysRevA.109.L030601 for further discussions on the ground state configuration and operator choices with and

without interaction, numerical issues related to particle choice at near-half-filling for odd lattice size, robustness of temporal scalings, and for additional plots and related discussions on the dynamics of the quantum Fisher information corresponding to the charge density wave (CDW) operator.

[101] S. R. White and A. E. Feiguin, Real-time evolution using the density matrix renormalization group, Phys. Rev. Lett. **93**, 076401 (2004).

[102] U. Schollwöck, The density-matrix renormalization group in the age of matrix product states, Ann. Phys. **326**, 96 (2011).

[103] As we impose periodic boundary condition (PBCs), the convergence in the MPS bond dimension is more costly compared to that of open boundary condition (OBCs). The truncation error achievable by m bond dimension in OBC requires m^2 bond dimension in PBC. The interacting analysis is naturally restricted to small system sizes, and few available data points available from the Fibonacci series are not sufficient for a proper scaling analysis. However, through a comparative analysis between the NI and the interacting systems in the context of QFI, we find that the role of interaction remains minimal, while fermionic statistics, the manifestation of which comes in the form of a proper antisymmetrization of the single-particle eigenstates, plays the major role in the observed many-body effects.

[104] It can be shown that the time evolution of QFI under a generic Hamiltonian of the form $\hat{H} = \hat{H}_1 + V\hat{H}_2$ has a quadratic dependence in time: $F_Q \sim t^2(\langle\overline{(\hat{\mathcal{H}}_2)_t}^2\rangle - |\langle\overline{(\hat{\mathcal{H}}_2)_t}\rangle|^2)$, where $\overline{(\hat{\mathcal{H}}_2)_t} = \frac{1}{t}\int_0^t \hat{H}_2(t')dt'$ [105–107].

[105] S. Pang and T. A. Brun, Quantum metrology for a general Hamiltonian parameter, Phys. Rev. A **90**, 022117 (2014).

[106] M. Skotiniotis, P. Sekatski, and W. Dür, Quantum metrology for the Ising Hamiltonian with transverse magnetic field, New J. Phys. **17**, 073032 (2015).

[107] Q. Guan and R. J. Lewis-Swan, Identifying and harnessing dynamical phase transitions for quantum-enhanced sensing, Phys. Rev. Res. **3**, 033199 (2021).